Advanced Composite Materials
Publication details, including instructions for authors and subscription information:
http://www.tandfonline.com/loi/tacm20

Taguchi's Approach to Examine the Effect of Drilling Induced Damage on the Notched Tensile Strength of Woven GFR-epoxy Composites

T. Parameshwaranpillai [a], P. R. Lakshminarayanan [b] & B. Nageswara Rao [c]

[a] Faculty of Automobile Engineering, Anna University, Tirichirappalli-620 024, India

[b] Faculty of Manufacturing Engineering, Annamalai University, Chidambaram-608 002, India

[c] Structural Analysis and Testing Group, Vikram Sarabhai Space Centre, Trivandrum-695 022, India;, Email: bnrao52@rediffmail.com

Version of record first published: 02 Apr 2012.

To cite this article: T. Parameshwaranpillai , P. R. Lakshminarayanan & B. Nageswara Rao (2011): Taguchi's Approach to Examine the Effect of Drilling Induced Damage on the Notched Tensile Strength of Woven GFR-epoxy Composites, Advanced Composite Materials, 20:3, 261-275

To link to this article: http://dx.doi.org/10.1163/092430410X547083

///VSP///

Advanced Composite Materials 20 (2011) 261–275

ADVANCED COMPOSITE MATERIALS
brill.nl/acm

Taguchi's Approach to Examine the Effect of Drilling Induced Damage on the Notched Tensile Strength of Woven GFR–epoxy Composites

T. Parameshwaranpillai [a], **P. R. Lakshminarayanan** [b] **and B. Nageswara Rao** [c,*]

[a] Faculty of Automobile Engineering, Anna University, Tirichirappalli-620 024, India
[b] Faculty of Manufacturing Engineering, Annamalai University, Chidambaram-608 002, India
[c] Structural Analysis and Testing Group, Vikram Sarabhai Space Centre, Trivandrum-695 022, India

Received 10 February 2010; accepted 3 November 2010

Abstract

Drilling of holes into laminates is essential to facilitate bolting or riveting to the main load-bearing structures. Delamination is the most evident damage that can be generated during the drilling of a laminate. This paper presents the design of experiments and analysis of variance (ANOVA) techniques of Taguchi useful in examining the effect of drilling induced damage on the notched tensile strength of woven GFR–epoxy composites. Fracture data of center-hole tensile specimens are correlated using a modification in the inherent flaw model.

Keywords

Woven GFR–epoxy composites, notched tensile strength, inherent flaw model, analysis of variance (ANOVA), Taguchi technique

1. Introduction

Composite materials are widely used in structural applications. It has become necessary to drill holes into the laminates to facilitate bolting or riveting to the main load-bearing structures. Delamination is the most evident damage that can be generated during the drilling of a laminate. Hocheng and Tsao [1, 2] have presented a comprehensive analysis of delamination in use of various drill types and predicted the critical thrust force at the onset of delamination. Stress concentration, delamination and microcracking associated with drilled holes significantly reduce the performance of composites [3–7]. Srinivasa Rao *et al.* [8] have performed an experimental study to analyze the influence of drilling parameters on the extension

* To whom correspondence should be addressed. E-mail: bnrao52@rediffmail.com
Edited by the JSCM

 DOI:10.1163/092430410X547083

of the damage and to evaluate the notched tensile strength and pin-bearing strength of the woven glass fiber reinforced (GFR)–epoxy composite laminates.

This paper presents the design of experiments and analysis of variance (ANOVA) techniques of Taguchi useful in examining the effect of drilling induced damage on the notched tensile strength of woven GFR–epoxy composites. Finally, the fracture data of center-hole tensile specimens are correlated using a modification in the inherent flaw model.

2. Design of Experiments and Analysis of Variance (ANOVA) Techniques of Taguchi

Many processes typically have a large number of factors or parameters that influence the final outcome. Identification of their individual contributions and their intricate relationship in development of such processes is possible through design of experiments. The concept of experimental design involving multiple factors was first introduced by Sir Ronald Fisher nearly 70 years ago. The technique is known as a factorial design of experiments. It is also called a matrix experiment. Taguchi has established an orthogonal array (OA) to describe a large number of experimental situations. Orthogonal arrays have been investigated by many other researchers [9–11]. Taguchi's approach complements three important areas. First, Taguchi clearly defined a set of orthogonal arrays, each of which can be used for many situations. Second, he has devised a standard method for analyzing the results. Third, he has developed a graphical tool, called linear graphs. Taguchi's approach of combining standard experimental design techniques and analysis methods produces consistency and reproducibility rarely found in any other statistical method [12]. The real power of an orthogonal array is its ability to evaluate several factors with a minimum of trials or experiments. Much information can be obtained from few tests.

The design of an experiment involves: selection of independent variables (factors); selection of a number of level settings for each independent variable; selection of the orthogonal array; assignment of an independent variable to each column of the orthogonal array; conducting numerical simulations. To implement orthogonal arrays on the computer, an algorithm is developed to create orthogonal arrays for three-level parameters. These are the arrays L_9, L_{27}, L_{81} which are used for 4, 13 or 40 parameters, respectively. The basic information is provided by a Latin Square which presents the smallest orthogonal entities. When there is a complete orthogonal system of $(n-1)$ Latin Square of dimensions $n \times n$ denoted by $L_1, L_2, \ldots, L_{n-1}$, it is possible to construct an orthogonal array of size n^r $(r = 2, 3, \ldots)$ with the number of columns $(n^r - 1/n - 1)$. The number r represents the number of trials.

In constructing an orthogonal array for a k-level system, Bose and Bush [13] have shown a method of using a matrix whose elements are taken cyclically, Masuyama [14] has used the theory of algebraic numbers for the first time in constructing orthogonal arrays. The three mentioned arrays L_9, L_{27} and L_{81} are basically built from two Latin Squares of dimension 3 × 3. L_9 is created from the Latin Square, L_{27} from L_9, and L_{81} from L_{27}. Singaravelu *et al.* [15] have provided the listing of the computer program for the generation of three arrays L_9, L_{27} and L_{81}. The L_{81} and other standard OAs can also be found in reference [16].

Before selecting an orthogonal array, the minimum number of simulations to be carried out is:

$$N_{\text{Taguchi}} = 1 + \text{Number of factors} \times \text{Degrees of freedom (DOF)}. \qquad (1)$$

Once the orthogonal array is selected, the experiments are conducted as per the level combinations. The performance parameter (output) is noted down for each experimental run for analysis. Since each experiment is the combination of different factor levels, it is essential to segregate the individual effect of independent variables. This is usually done by summing up the performance parameter values for the corresponding level setting and then evaluating the mean. Then, the sum of the squares of the deviation of each mean value from grand mean value is calculated. The sum of the squares of the deviation of a particular variable indicates whether the performance parameter is sensitive to the change of level of setting. The percentage contribution of an individual parameter is the sum of the squares of the individual parameters divided by the total sum of squares. Let, y_i be the output characteristics. The sum of the squares is the measure of the deviation from the mean value of the data. The effects of the factors can be estimated by summing the squares of the effects at various levels and averaging over the number of degrees of freedom. Thus, the total sum of the squares (total variation) is calculated from:

$$SS_{\text{T}} = \sum_{i=1}^{N} (y_i - \overline{T})^2 = \sum_{i=1}^{N} y_i^2 - \frac{T^2}{N} = \sum_{i=1}^{N} y_i^2 - CF. \qquad (2)$$

Here $\overline{T} = T/N$ is the mean value of the total data; $T = \sum_{i=1}^{N} y_i$ is the sum of the data (output characteristics); $CF = T^2/N$ is the correction factor and N is the total number of experiments.

The general formula for the sum of the squares due to a factor A is:

$$SS_{\text{A}} = \sum_{i=1}^{k_{\text{A}}} \frac{A_i^2}{n_{Ai}} - \frac{T^2}{N} = \sum_{i=1}^{k_{\text{A}}} n_{Ai} (\overline{A}_i - \overline{T})^2. \qquad (3)$$

Here k_{A} is the number of levels of factor A; A_i is the sum of observations under A_i level; $\overline{A}_i = A_i/n_{Ai}$ is the average of observations under A_i level and n_{Ai} is the number of observations under A_i level.

Percentage contribution of factor A to the total variation can be calculated from

$$P_{\text{A}} = 100 \times \frac{SS_{\text{A}}}{SS_{\text{T}}}. \qquad (4)$$

In the same way, the percentage contribution of each factor to the total variation can be calculated after determining the sum of the squares due to each factor. The above calculations indicate the factors which may affect the average response. Taguchi has created a transformation, namely, the signal-to-noise (S/N) ratio, which consolidates several repetitions (at least two data points are required) into one value and reflects the amount of variation present. There are several S/N ratios available depending on the type of output characteristic [17]:

Lower-is-better (LB):

$$S/N_{\mathrm{LB}} = -10\log_{10}\left[\frac{1}{n_r}\sum_{j=1}^{n_r} y_i^2(j)\right], \tag{5}$$

where n_r is the number of tests in a trial or number of repetitions regardless of noise levels.

Nominal-is-best (NB):

$$S/N_{\mathrm{NB1}} = -10\log_{10}(\sigma_i^2), \tag{6}$$

$$S/N_{\mathrm{NB2}} = 10\log_{10}\left(\frac{\mu_i^2}{\sigma_i^2} - \frac{1}{n_r}\right). \tag{7}$$

Here the mean (μ_i) and variance (σ_i^2) are defined as:

$$\mu_i = \frac{\sum_{j=1}^{n_r} y_i(j)}{n_r} \quad \text{and} \quad \sigma_i^2 = \frac{\sum_{j=1}^{n_r}(y_i(j) - \mu_i)^2}{n_r - 1}. \tag{8}$$

Higher-is-better (HB):

$$S/N_{\mathrm{HB}} = -10\log_{10}\left[\frac{1}{n_r}\sum_{j=1}^{n_{r_r}} \frac{1}{y_i^2(j)}\right]. \tag{9}$$

The LB and HB S/N ratios are both easy to calculate. The S/N for NB1 is a function of variation only, whereas, S/N for NB2 is a function of both average and variation. A standard ANOVA can be done on the S/N ratio which will identify factors significant in increasing the average value of S/N and subsequently reducing variation. The influential factors are the only ones necessary to have the set level or controlled. The non-influential factors should be set at the lowest level. A confirmation experiment is essential to demonstrate the chosen factors and levels.

Woven glass/epoxy laminates containing 16 layers were prepared using hand lay-up technique with 45% fiber volume fraction (V_{f}) and cut into specimens for notched tensile strength evaluation [8]. The influence of drilling parameters on the extension of delamination is examined by conducting the number of experiments as per the design of experiments and analysis of variance (ANOVA) techniques of Taguchi. In the plan of experiments, three factors (feed rate, spindle speed and drill diameter) were selected at three levels. The minimum number of experiments to be conducted for selecting an orthogonal array is 7. The orthogonal array chosen was the L_9 (3^4). Initially, the plan of experiments in Table 1 was made of nine tests only. Drilling operations were conducted using a standard twist drill having 118° drill

Table 1.
Orthogonal array L_9 (3^4) of Taguchi and values of delamination factor (F_d), maximum diameter of the delamination zone (D_{max}) and notched tensile strength (σ_{Nh})

Test runs	Feed rate, f (mm/rev)	Spindle speed, N (rpm)	Drill diameter, D (mm)	D_{max} (mm)	Notched tensile strength, σ_{Nh} (MPa)	Delamination factor, F_d	F_d equation (11)	Relative error (%)
1	0.0635	500	6	6.833	152.63	1.139	1.142	−0.2
2	0.0635	710	8	9.125	145.61	1.141	1.145	−0.4
3	0.0635	1000	10	11.43	128.07	1.143	1.148	−0.4
4	0.1016	500	8	9.241	122.36	1.155	1.148	0.7
5	0.1016	710	10	11.59	123.68	1.159	1.150	0.8
6	0.1016	1000	6	6.977	145.17	1.163	1.158	0.4
7	0.254	500	10	11.73	119.73	1.173	1.176	−0.3
8	0.254	710	6	7.093	125.26	1.182	1.183	−0.1
9	0.254	1000	8	9.512	119.29	1.189	1.186	0.2
10	0.1016	355	10	11.45	124.38	1.145	1.144	0.1
11	0.254	1000	10	11.83	105.70	1.183	1.185	−0.2
12	0.254	710	8	9.472	131.58	1.184	1.182	0.2

point angle, 22° helix angle and 51° chisel angle. Both back and top surface plates having 12 mm hole-diameter were used during drilling. Totally, three drill bits were used and with each drill bit, three holes were made. Figure 1 shows the experimental setup including the standard twist drill, dimensions of the test coupons. The drilled-hole specimens are scanned using the AutoCAD drawing technique [18] to measure the damage around the hole.

The delamination factor (F_d) is defined as:

$$F_d = D_{max}/D, \tag{10}$$

in which D_{max} is the maximum diameter of the delamination zone and D is the hole diameter as shown in Fig. 2. The first nine values of the delamination factor (F_d) in Table 1 are considered for ANOVA. The most important parameter affecting the delamination factor is the feed rate (94.36%). The other parameters *viz.* spindle speed and drill diameter affecting the delamination factor are 4.87% and 0.77%, respectively. Using the multi-variable linear regression analysis, the correlation between delamination factor (F_d) and cutting parameters, namely, feed rate (f, in mm/rev), spindle speed (N, in rpm) in drilling (with the regression coefficient, $R^2 = 0.923242$) is obtained from the first nine data points in Table 1 as [8]:

$$F_d = 1.125814 + 0.19432f + 1.827 \times 10^{-5}N - 7.6 \times 10^{-4}D. \tag{11}$$

The advantage of the Taguchi method utilizing orthogonal arrays is to study a large number of variables with a small number of experiments, which provide full information of all the parameters that affect the performance. Equation (11) is valid

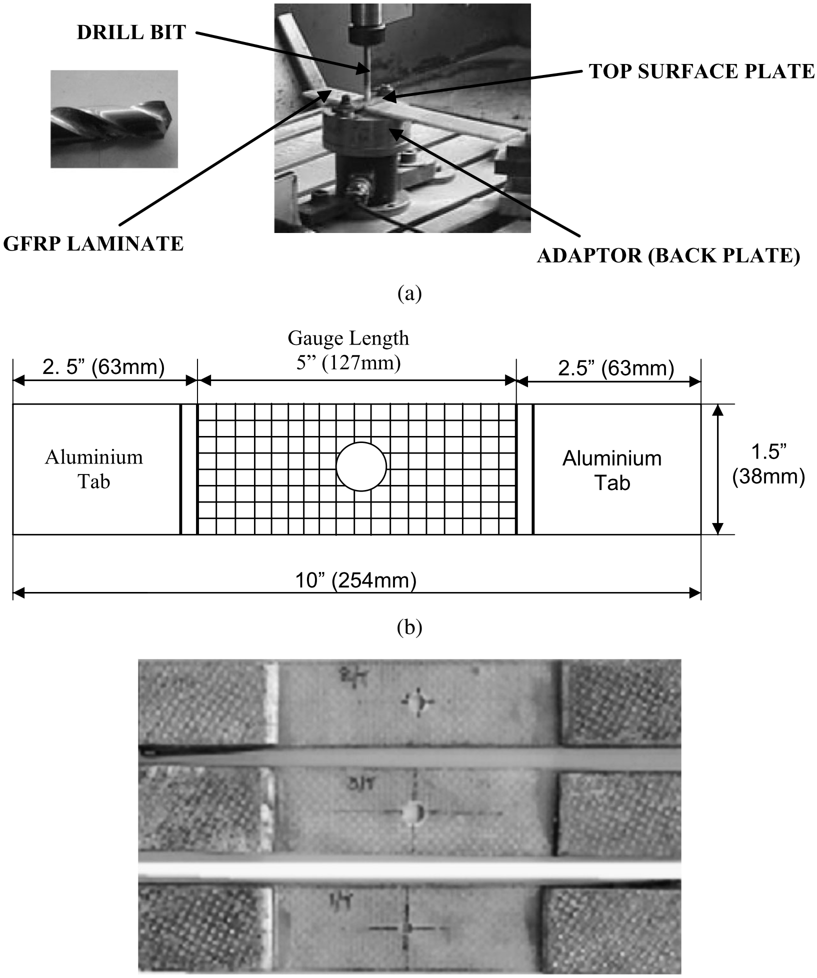

Figure 1. Experimental setup for drilling operation, dimensions of the test coupons. (a) Experimental setup, (b) specimen with a central hole and (c) test coupons having 8, 10 and 6 mm center-hole diameter.

for any level between the lower and higher level of the influencing factors. To confirm further, three more specimens were drilled with different machining parameters (test runs 10–12 in Table 1). The higher levels of the influencing factor (i.e., feed rate, f) and other levels of the non-influencing factors (i.e., spindle speed, N and the drill diameter, D) are chosen while performing the confirmation experiments. The non-influential spindle speed (N) is intentionally specified at a value less than its lower level in test run-10 to confirm the validity of equation (11). The results of F_d obtained from the expression (11) are found to be within $\pm 1\%$ of the measured values.

Tests were conducted for notched tensile strength (σ_{Nh}) evaluation of the twelve drilled specimens [8] and the test results are presented in Table 1. The details of modifications made in the inherent flaw model for accurate evaluation of the notched tensile strength of the drilled specimens are presented in the forthcoming section. A few more specimens were drilled with machining parameters as specified in test runs 1–9 of Table 1 and a negligible variation was found in the delamination factor (F_d). Hence, analysis of variance (ANOVA) on the S/N ratio does not show any significant difference on the percentage contribution of the influencing machining parameters. These specimens were used for evaluation of notched shear and pin bearing strengths of woven GFR–epoxy composites.

3. Notched Tensile Strength of Laminates

Fracture behavior of drilled center-hole tensile specimens with drilling damage has been examined using the modified inherent flaw model.

The inherent flaw model consists of a hole from which two intense energy regions are modeled as cracks that have a small but finite length 'a_{hi}' (see Fig. 3). The length 'a_{hi}' is taken to be the characteristic length of an inherent flaw. The assumption is made of an inherent flaw in the wide tensile specimen (the width of the specimen is assumed to be infinitely large) having a center circular hole with edge cracks at the ends of its diameter.

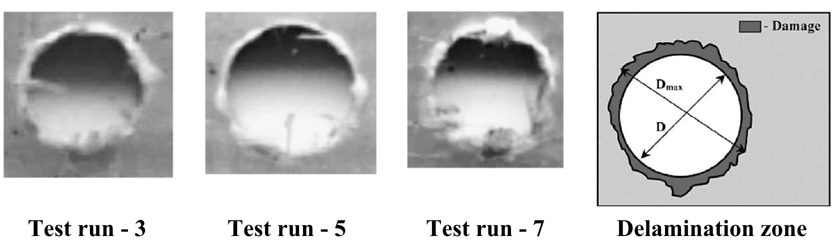

Figure 2. Scanned views of drilling induced delaminations for different machining conditions of the test runs.

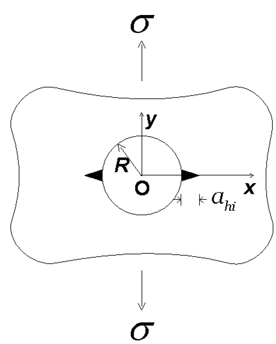

Figure 3. Inherent flaw length (a_{hi}) in a center-hole wide tensile panel.

For the case of the un-notched tensile specimen, the assumption of an inherent flaw represents the case of a center crack tension specimen (having crack length '$2a_{\mathrm{hi}}$'). Waddoups *et al.* [19] have considered the stress intensity factors for these two cracked configurations. The inherent flaw size is estimated by equating the critical stress intensity of these two cracked configurations utilizing the notched and un-notched tensile strength values.

The stress intensity factor for a wide tensile specimen having center crack is:

$$K_{\mathrm{I}} = \sigma\sqrt{\pi c}, \tag{12}$$

where σ the applied stress and c is is half the crack length.

The stress intensity factor for a wide tensile specimen having center hole with edge cracks is:

$$K_{\mathrm{I}} = \sigma\sqrt{\pi c}\, f\left(\frac{c}{R}\right), \tag{13}$$

where σ is the applied stress; c is the length of the crack at the hole-diameter ends and R is the hole-radius.

An approximation for the function $f(c/R)$ in equation (13) is given by [20]:

$$f\left(\frac{c}{R}\right) = \frac{0.6866}{0.2772 + c/R} + 0.9439. \tag{14}$$

For the known inherent flaw size, the critical stress intensity factor ($K_{\mathrm{Q}\infty}$) can be obtained directly from equation (12) using $\sigma = \sigma_0$ and $c = a_{\mathrm{hi}}$. Here σ_0 is the un-notched tensile strength. The value of $K_{\mathrm{Q}\infty}$ can also be obtained from equation (13) using the notched strength ($\sigma_{\mathrm{Nh}}^{\infty}$) for σ and a_{hi} for c. Since a_{hi} is unknown, one can obtain by equating these two critical stress intensity factors: $K_{\mathrm{Q}\infty} = \sigma_0\sqrt{\pi a_{\mathrm{hi}}} = \sigma_{\mathrm{Nh}}^{\infty}\sqrt{\pi a_{\mathrm{hi}}}\, f(a_{\mathrm{hi}}/R)$, which implies that

$$f\left(\frac{a_{\mathrm{hi}}}{R}\right) = \frac{\sigma_0}{\sigma_{\mathrm{Nh}}^{\infty}}. \tag{15}$$

The notched strength ($\sigma_{\mathrm{Nh}}^{\infty}$) of the center circular hole wide tensile specimen is obtained from the experimental notched strength (σ_{Nh}) of the finite width tensile specimen by multiplying the correction factor [21]:

$$\frac{K_{\mathrm{T}}^{\infty}}{K_{\mathrm{T}}} = \alpha + \frac{1}{2}\left(K_{\mathrm{T}}^{\infty} - 3\right)(1 - \beta)\beta^3, \tag{16}$$

where the stress concentration factor for an infinite width plate:

$$K_{\mathrm{T}}^{\infty} = 1 + \sqrt{2\left(\sqrt{\frac{E_{yy}}{E_{xx}}} - \nu_{yx}\right) + \frac{E_{yy}}{G_{xy}}}, \tag{17}$$

$$\alpha = 3\left(1 - \frac{D}{W}\right)\left\{2 + \left(1 - \frac{D}{W}\right)^3\right\}^{-1}, \qquad \beta = \frac{1}{2}\left(\sqrt{9 - 8\alpha} - 1\right),$$

$D = 2R$ is the hole-diameter, W is the specimen width. E_{xx}, E_{yy} and G_{xy} are the axial, transverse and shear moduli respectively and ν_{xy} is the major Poisson's ratio for the laminate, and $\nu_{yx} = (E_{yy}/E_{xx})\nu_{xy}$.

Using $\sigma_{\mathrm{Nh}}^{\infty}$, σ_0 and R, the unknown characteristic length, a_{hi} is found from equations (14) and (15) as:

$$a_{\mathrm{hi}} = R\left\{0.6866\left(\frac{\sigma_0}{\sigma_{\mathrm{Nh}}^{\infty}} - 0.9439\right)^{-1} - 0.2772\right\}. \tag{18}$$

After determining the characteristic length (a_{hi}), the fracture strength ($\sigma_{\mathrm{Nh}}^{\infty}$) can be obtained directly from equation (15) specifying the hole-diameter, D $(=2R)$. Fracture strength (σ_{Nh}) of the finite width plate can be obtained by dividing the determined $\sigma_{\mathrm{Nh}}^{\infty}$ with the correction factor, $K_{\mathrm{T}}^{\infty}/K_{\mathrm{T}}$ from equation (16). It is noted from the fracture data on different materials that the fracture strength decreases with increase in the hole-diameter. Equation (18) indicates that the characteristic length (a_{hi}) is not a material constant. It increases with increase in the hole-diameter. This calls for a modification in the inherent flaw model.

From the above observations one can write a relation between a_{hi} and $\sigma_{\mathrm{Nh}}^{\infty}$ in the non-dimensional form as:

$$a_{\mathrm{hi}} = a^*\left(1 - m\frac{\sigma_{\mathrm{Nh}}^{\infty}}{\sigma_0}\right)^2. \tag{19}$$

The parameters a^* and m in equation (19) are to be determined by a least square curve fit to the data for a_{hi} and $\sigma_{\mathrm{Nh}}^{\infty}/\sigma_0$. For the determination of these parameters, two center-hole specimen tests in addition to the un-notched strength of the material are required; normally more tests are performed to take scatter in test results into account. It should be noted that $m = 0$ in equation (19) represents the case of constant damage size as per the original inherent flaw model [19]. For the case: $m > 1$ and $\sigma_{\mathrm{Nh}}^{\infty} = \sigma_0$, equation (19) results in the value of $a^* < 0$. Hence, the variation of the parameter in equation (19) can be $0 \leqslant m \leqslant 1$. Whenever m is found to be greater than unity, the parameter m has to be truncated to 1 by suitably modifying the parameter a^* with the fracture data. If m is found to be less than zero, the parameter m has to be truncated to zero and the average of a_{hi} values from the fracture data yields the parameter a^*.

Once a^* and m in equation (19) are known, it is possible to eliminate the characteristic length (a_{hi}) from the fracture strength equation (15). The resulting nonlinear equation for the fracture strength ($\sigma_{\mathrm{Nh}}^{\infty}$) is:

$$\left\{1 - 0.9439\frac{\sigma_{\mathrm{Nh}}^{\infty}}{\sigma_0}\right\}\left\{\frac{a^*}{R}\left(1 - m\frac{\sigma_{\mathrm{Nh}}^{\infty}}{\sigma_0}\right)^2 + 0.2772\right\} - 0.6866\frac{\sigma_{\mathrm{Nh}}^{\infty}}{\sigma_0} = 0. \tag{20}$$

This non-linear fracture strength equation (20) is solved using the Newton–Raphson iterative scheme to obtain $\sigma_{\mathrm{Nh}}^{\infty}$ for the specified hole-diameter. The fracture strength (σ_{Nh}) of the finite width plate is obtained by dividing the determined $\sigma_{\mathrm{Nh}}^{\infty}$ with the correction factor, $K_{\mathrm{T}}^{\infty}/K_{\mathrm{T}}$ from equation (16).

4. Results and Discussion

Mechanical as well as the notched tensile strength properties of the woven glass fiber reinforced (GFR)–epoxy cross-ply laminates are presented in Table 2. As expected, the notched strength decreases with increase in the hole diameter. Considering the average enhanced diameters of the drilled holes and the respective notched strength values, the fracture parameters a^* and m in equation (19) determined are: $a^* = 17.2$ mm and $m = 0.862$. Notched tensile strength (gross) values evaluated in Table 2 for the measured enhanced diameters ($D_{\max}$) of the drilled central-hole specimens are found to be in reasonably good agreement with the test results [8]. Figure 4 shows a good comparison of tensile fracture strength (σ_{Nh}) estimated for the measured and fitted maximum diameter ($D_{\max}$) of the delamination zone for twelve different machining conditions. Figure 5 shows the tensile fracture strength variation with the center-hole diameter of 38 mm wide woven glass fiber reinforced (GFR)–epoxy cross-ply laminates along with the test data.

Ramesh Kumar [22] has carried out an experimental investigation to study the effect of drilling on the strength properties of the woven GFR–epoxy composites. Srinivasa Rao [23] has performed fracture analysis utilizing the modified point stress criterion. Figure 6 shows the comparison of the notched tensile strength values obtained from the present modified inherent flaw model with those of test

Table 2.
Mechanical as well as notched tensile strength properties of the Woven glass fiber reinforced (GFR)–epoxy cross-ply laminates [8] and comparison of notched tensile strength test values with those obtained from the modified inherent flaw model

Test runs	Feed rate, f (mm/rev)	Spindle speed, N (rpm)	Drill diameter, D (mm)	$D_{\max}$ (mm)	Notched tensile strength, σ_{Nh} (MPa)	Modified inherent flaw model σ_{Nh} (MPa)	Relative error (%)
1	0.0635	500	6	6.833	152.63	144.29	5.4
2	0.0635	710	8	9.125	145.61	133.17	8.5
3	0.0635	1000	10	11.43	128.07	122.54	4.3
4	0.1016	500	8	9.241	122.36	132.63	−8.4
5	0.1016	710	10	11.59	123.68	121.81	1.5
6	0.1016	1000	6	6.977	145.17	145.17	1.1
7	0.254	500	10	11.73	119.73	121.16	−1.2
8	0.254	710	6	7.093	125.26	142.98	−14.2
9	0.254	1000	8	9.512	119.29	131.37	−10.1
10	0.1016	355	10	11.45	124.38	122.44	1.6
11	0.254	1000	10	11.83	105.70	120.71	−14.2
12	0.254	710	8	9.472	131.58	131.55	0.0

$E_{xx} = E_{yy} = 20.59$ GPa; $\nu_{xy} = 0.1124$; $G_{xy} = 10.87$ GPa; $\sigma_0 = 226.3$ MPa; $W = 38$ mm.

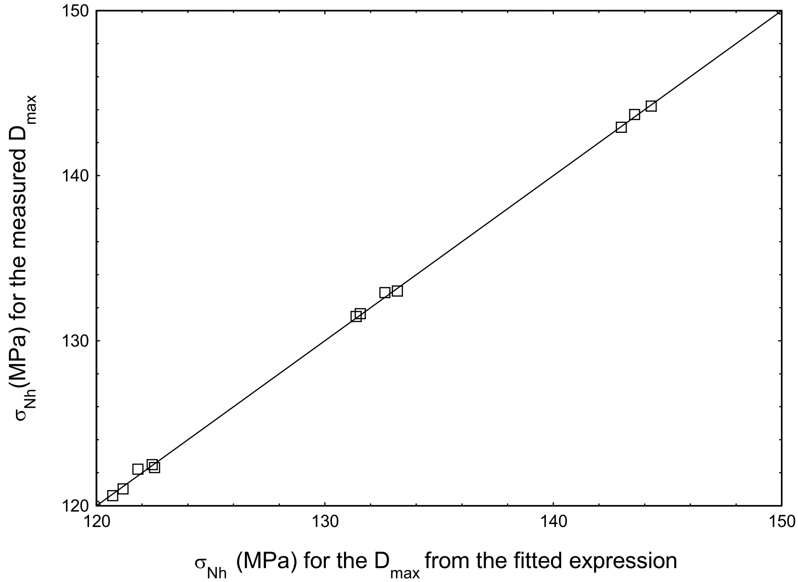

Figure 4. Comparison of tensile fracture strength (σ_{Nh}) estimated for the measured and fitted maximum diameter (D_{max}) of the delamination zone for twelve different machining conditions.

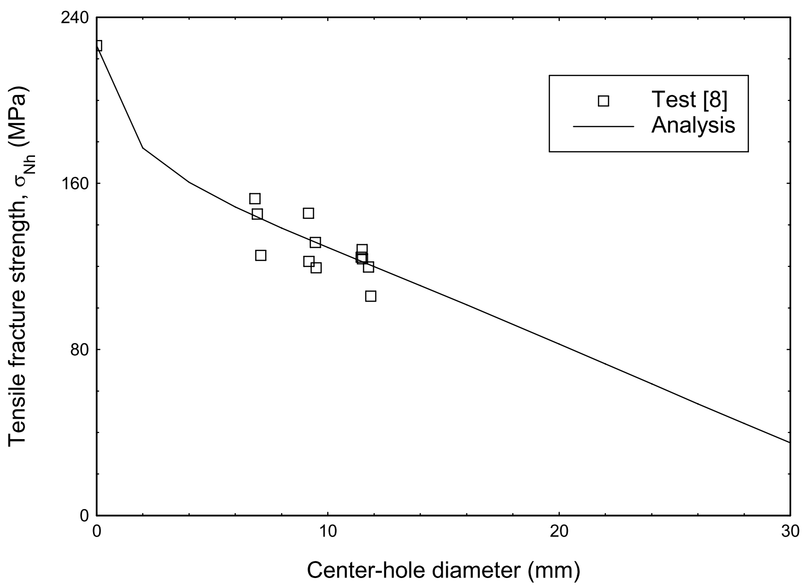

Figure 5. Tensile fracture strength variation with the center-hole diameter of 38 mm wide woven glass fiber reinforced (GFR)–epoxy cross-ply laminates.

results [22] and the fracture analysis results [23]. The woven fabric laminate is cut in ±45° direction and performed uniaxial tension test to obtain the shear strength

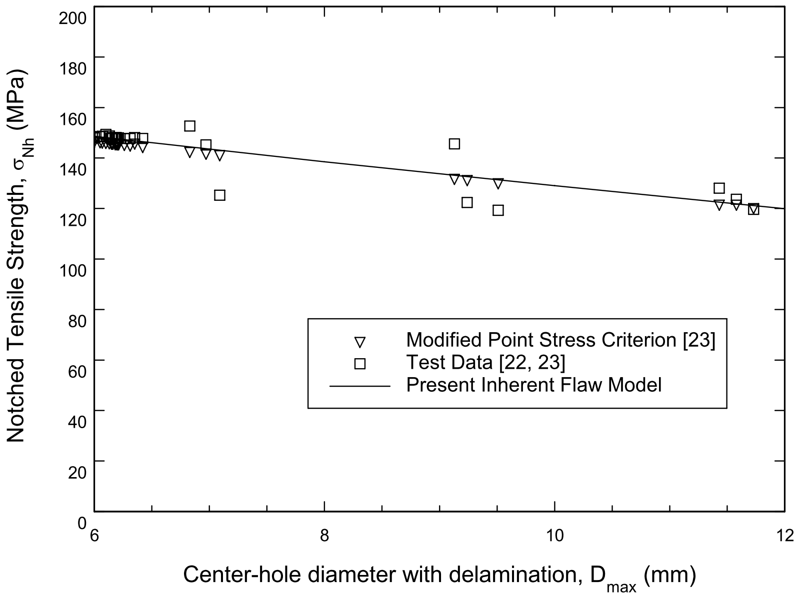

Figure 6. Comparison of notched tensile strength estimates with test data of woven glass fiber reinforced epoxy cross-ply laminates having center holes.

Table 3.
Notched tensile strength (σ_{Nh}) of the woven fabric laminates cut in ±45° direction and performed uniaxial tension tests to obtain shear strength properties

No.	Feed rate, f (mm/rev)	Spindle speed, N (rpm)	Drill diameter, D (mm)	D_{max} (mm)	In-plane shear strength, σ_{Nh} (MPa) [23]	Modified inherent flaw model σ_{Nh} (MPa)	Relative error (%)
1	0.0635	710	8	9.13	57.8	57.19	1.1
2	0.1016	500	8	9.24	57.0	57.01	0.1
3	0.2540	1000	8	9.51	54.4	56.57	−4.0
4	0.0635	1000	10	11.43	56.7	53.36	5.9
5	0.1016	710	10	11.58	54.2	53.10	2.0
6	0.2540	500	10	11.73	50.6	52.84	−4.4

$E_{xx} = E_{yy} = 7.784$ GPa; $\nu_{xy} = 0.6863$; $G_{xy} = 10.87$ GPa; $\sigma_0 = 84.1$ MPa; $a^* = 81.5$ mm; $m = 1$; width, $W = 38$ mm.

properties of GFRP laminates. Table 3 gives a comparison of the notched shear strength of GFRP laminates with the present modified inherent flaw model. The analysis results are found to be in good agreement with test results [23]. Table 4 gives comparison of the present analysis results with test results [7] of notched tensile strength of continuous fiber impregnated thermoplastic (COFIT) plain weave

Table 4.
Notched tensile strength of COFIT plain weave composites with conventional hole-drilling and orbital hole-drilling

Hole diameter, D (mm)	Notched tensile strength, σ_{Nh} (MPa)				
	Mariatti *et al.* [7]			Present study	
	Test	Analysis	Relative error (%)	Analysis	Relative error (%)
Conventional hole-drilling: $a^* = 15.2$ mm; $m = 0$					
6	230.1	213.2	7.3	214.78	6.6
8	214.8	199.4	7.2	206.45	3.9
10	194.5	185.6	9.7	197.86	−1.7
14	179.8	160.7	10.6	179.8	0.0
Orbital hole-drilling: $a^* = 45.5$ mm; $m = 0$					
6	229.0	226.1	1.3	237.78	−3.9
8	233.9	218.4	6.6	231.38	1.1
10	227.9	209.9	7.9	224.22	1.6
14	217.7	192.0	11.8	207.8	4.6

$E_{xx} = 9.222$ GPa; $E_{yy} = 9.347$ GPa; $\nu_{xy} = 0.21$; $G_{xy} = 5.334$ GPa; $\sigma_0 = 238.7$ MPa; length, $L = 210$ mm; width, $W = 50$ mm.

composites. The notched tensile strength properties of laminate with orbital hole-drilling shows better damage resistance than those of conventional hole-drilling. Table 5 gives a good comparison of off-axis notched tensile strength estimates of fiber-metal (GALRE-3) laminates of different orientations with test results [24]. The notch sensitivity in GALRE-3 is found to be highest in the fiber direction, and it decreases with increasing fiber orientation angle to the lowest in the 45° direction.

5. Conclusions

The damage induced during drilling of GFRP laminates is quantified in terms of a delamination factor (F_d). The analysis of variance (ANOVA) approach of Tauguchi is used to identify the most dominant factor in producing damage. The feed rate is found to be the factor that contributes most to drilling damage. To minimize drilling damage, low feed rates are preferred in drilling of composite laminates. The delamination factor is correlated with drilling parameters (feed rate, spindle speed and drill diameter). The notched tensile strength of center-hole specimens predicted well the test results using the modified inherent flaw model. The notched tensile strength estimates of COFIT plain weave composites and GLARE-3 laminates having different fiber orientation are found to be in good agreement with test results.

Table 5.
Off-axis notched strengths for center open hole specimens of GLARE-3 laminate of different fiber orientations (θ) (width, $W = 20$ mm)

Hole diameter, D (mm)	Notched tensile strength, σ_{Nh} (MPa)		
	Test [24]	Analysis	Relative error (%)
$\theta = 0°$; $E_{xx} = 58.4$ GPa; $E_{yy} = 58.7$ GPa; $\nu_{xy} = 0.279$; $G_{xy} = 18.9$ GPa; $\sigma_0 = 685.5$ MPa; $a^* = 4.15$ mm; $m = 0.742$			
2.02	458.5	459.82	−0.3
4.0	391.2	389.03	0.6
8.03	283.8	284.53	−0.3
$\theta = 5°$; $E_{xx} = 58.21$ GPa; $E_{yy} = 58.5$ GPa; $\nu_{xy} = 0.2815$; $G_{xy} = 19.02$ GPa; $\sigma_0 = 637.8$ MPa; $a^* = 5.52$ mm; $m = 0.775$			
2.0	442.7	442.7	0.0
4.0	377.4	337.39	0.0
7.93	280.2	280.2	0.0
$\theta = 15°$; $E_{xx} = 56.76$ GPa; $E_{yy} = 57.0$ GPa; $\nu_{xy} = 0.2995$; $G_{xy} = 19.81$ GPa; $\sigma_0 = 539.9$ MPa; $a^* = 7.19$ mm; $m = 0.680$			
2.0	408.2	410.3	−0.5
4.0	355.0	351.58	1.0
7.97	259.1	260.25	−0.4
$\theta = 30°$; $E_{xx} = 53.35$ GPa; $E_{yy} = 53.49$ GPa; $\nu_{xy} = 0.3423$; $G_{xy} = 21.88$ GPa; $\sigma_0 = 451.5$ MPa; $a^* = 12.88$ mm; $m = 0.854$			
2.02	341.2	339.53	0.5
4.0	294.2	297.91	−1.3
7.97	227.4	225.79	0.7
$\theta = 45°$; $E_{xx} = 51.6$ GPa; $E_{yy} = 51.6$ GPa; $\nu_{xy} = 0.3652$; $G_{xy} = 22.88$ GPa; $\sigma_0 = 431.2$ MPa; $a^* = 18.0$ mm; $m = 0.898$			
2.06	326.2	328.47	−0.7
4.0	295.2	291.92	1.1
7.91	223.7	224.68	−0.4

References

1. H. Hocheng and C. C. Tsao, Comprehensive analysis of delamination in drilling of composite materials with various drill bits, *J. Mater. Proc. Technol.* **140**, 335–339 (2003).
2. C. C. Tsao and H. Hocheng, Taguchi analysis of delamination associated with various drill bits in drilling of composite materials, *Intl J. Machines Tools Manuf.* **44**, 1085–1090 (2004).
3. S. D. Andrews, O. Ochoa and S. D. Owens, The effect of fastener hole defects, *J. Compos. Mater.* **27**, 3–20 (1993).
4. K. Y. Park, J. H. Choi and D. G. Lee, Delamination free and high efficiency drilling of carbon fiber reinforced plastics, *J. Compos. Mater.* **29**, 1988–2002 (1995).
5. U. A. Khashaba, Notched and pin bearing strengths of the GFRP composite laminates, *J. Compos. Mater.* **30**, 2042–2055 (1996).
6. A. B. Morais, Open-hole tensile strength of quasi-isotropic laminates, *Compos. Sci. Technol.* **60**, 1997–2004 (2000).

7. M. Mariatti, M. Nasir, H. Ismail and J. Backlund, Effect of hole drilling techniques on tensile properties of continuous fiber impregnated thermoplastic (COFIT) plain weave composites, *J. Reinf. Plast. Compos.* **23**, 1173–1186 (2004).
8. B. Srinivasa Rao, R. Rudramoorthy, S. Srinivas and B. Nageswara Rao, Effect of drilling induced damage on notched tensile and pin bearing strengths of woven GFR-epoxy composites, *Mater. Sci. Engng A* **472**, 347–352 (2008).
9. S. Addelman, Orthogonal main effect plans for asymmetrical factorial experiments, *Technometrics* **4**, 21–46 (1962).
10. O. Kempthorne, *The Design and Analysis of Experiments*. Robert E. Krieger Publishing, New York, USA (1979).
11. E. Seiden, On the problem of constructing orthogonal arrays, *Ann. Mathemat. Stat.* **25**, 151–156 (1954).
12. K. R. Ranjit, *A Primer on the Taguchi Method*, pp. 42–125. Society of Manufacturing Engineers Dearborn, Michigan, USA (1990).
13. R. C. Bose and K. A. Bush, Orthogonal arrays of strength two and three, *Ann. Mathemat. Stat.* **23**, 508–524 (1952).
14. M. Masuyama, On different sets for constructing orthogonal arrays of index two and of strength two, *Rep. Statist. Appl. Res. Un. Jap. Sci. Engng* **32**, 27–34 (1957).
15. J. Singaravelu, D. Jeyakumar and B. Nageswara Rao, Taguchi's approach for reliability and safety assessments in the stage separation process of a multistage launch vehicle, *Reliability Engng System Safety* **94**, 1526–1541 (2009).
16. G. Taguchi, *System of Experimental Design*. Kraus International Publications, New York, USA (1987).
17. P. J. Ross, *Taguchi Techniques for Quality Engineering*. McGraw-Hill, Singapore (1989).
18. U. A. Khashaba, Delamination in drilling GFR-thermoset composites, *Compos. Struct.* **63**, 313–327 (2004).
19. M. E. Waddoups, J. R. Eisenman and B. E. Kaminski, Macroscopic fracture mechanics of advanced composite materials, *J. Compos. Mater.* **5**, 446–451 (1971).
20. Effects of stress concentrations, in: *Composites Design Handbook for Space Structure Applications*, ESA-PSS-03-1101 (December, 1988).
21. S. C. Tan, Finite width correction factor for anisotropic plate containing central opening, *J. Compos. Mater.* **22**, 1080–1097 (1988).
22. A. Ramesh Kumar, An experimental investigation and analysis on the effect of drilling on the mechanical properties of composite laminates, *ME Thesis*, PSG College of Technology, Coimbatore, India (2004).
23. B. Srinivasa Rao, Fracture analysis on drilling induced damage of GFRP composite laminates, *ME Thesis*, PSG College of Technology, Coimbatore, India (2005).
24. M. Kawai and Y. Arai, Off-axis notched strength of fiber-metal laminates and a formula for predicting anisotropic size effect, *Composites: Part A* **40**, 1900–1910 (2009).